New insights into dissociation of deprotonated 2,4-dinitrotoluene by combined high-resolution mass spectrometry and density functional theory calculations: Dissociation of deprotonated 2,4-dinitrotoluene

Adrián Schwarzenberg, Jean-claude Tabet, Richard B. Cole, Xavier Machuron-mandard, Héloïse Dossmann

New insights into dissociation of deprotonated 2,4-dinitrotoluene by combined high resolution mass spectrometry and DFT calculations

Adrián Schwarzenberg[1], Jean-Claude Tabet[1], Richard B. Cole[1], Xavier Machuron-Mandard[2], Héloïse Dossmann[1*]

[1] UPMC, IPCM/CSOB, UMR 8232, 4 Place Jussieu, 75252 Paris Cedex, France
[2] CEA, DAM, DIF, 91297, Arpajon, France

Dear Editor,

Dinitrotoluene (DNT) compounds are nitroaromatic explosives and there are two isomers that are widely available: 2,4-dinitrotoluene (2,4-DNT) and 2,6-dinitrotoluene (2,6-DNT). These compounds are widely used in manufacturing explosives and propellants.[1] DNT is not found naturally in the environment, but its widespread uses have contributed to extensive contamination of rivers, lakes, soil, and groundwater.[2] The risk of carcinogenicity in humans underscores the importance of detecting these compounds.[3] Thus, DNT compounds have been studied by mass spectrometry (MS) under vacuum ionization conditions using electron ionization, thereby yielding mainly the radial $M^{\bullet-}$ anion *m/z* 182,[4] and then under atmospheric pressure ionization (API) conditions providing mainly the deprotonated molecules.[5] The analysis by electrospray ionization (ESI) in negative ion mode gives mainly $[M-H]^-$ at *m/z* 181. Upon fragmentation, deprotonated 2,4-DNT (**M_{181-1}**, **Figure 1a**) dissociates into the diagnostic *m/z* 116 fragment ion that we previously reported using ESI-high resolution MS/MS (HRMS/MS).[6] This diagnostic *m/z* 116 fragment ion was also observed under low temperature plasma (LTP) condition in low resolution MS/MS .[7] While HRMS/MS experiments do show that this ion is formed from the precursor $[M-H]^-$ by a formal loss of a neutral molecule whose formula is "H_3O_3N", the structure and route of formation of the diagnostic *m/z* 116 ion have not been described in detail. We have thus undertaken here the detailed study of the formation of the *m/z* 116 product ion by accurate mass measurements under high resolution and using density functional theory (DFT) calculations.

A standard solution (1 mg/mL in MeOH:ACN (1:1)) of 2,4-dinitrotoluene (2,4-DNT) (AccuStandard Europe, Niederbipp, Switzerland) was used. Samples were prepared by dilution at 1 µg mL^{-1} in H_2O/MeOH (1:1), then infused at a flow rate of 5 µL min^{-1} into an LTQ-Orbitrap

XL mass spectrometer (Thermo Fisher Scientific, Courtaboeuf, France) and ionized by ESI in the negative ion mode. The employed spray voltage was -2.5 kV giving in majority the deprotonated molecule $[M-H]^-$ at *m/z* 181 and the radical anion $[M]^{\bullet -}$ in minor abundance at *m/z* 182. Fragment ions were generated through resonant excitation by CID in the LTQ cell (30 ms activation time, 5 to 30 % normalized collision energies, NCE), and accurate mass measurements at high-resolution were acquired using the Orbitrap analyzer operated at 60,000 resolving power (FWHM) at *m/z* 400. To support experimental observations, electronic structure calculations have been performed using the GAUSSIAN 09[8] suite of programs. Geometry optimization and single point energy calculations were carried out with the OPBE functional[9] coupled to the 6-311++G(d,p) basis set.[10] Stationary points were characterized as minima (no imaginary frequencies) or as transition structures (one imaginary frequency) using vibrational frequency analysis. Computational results are detailed in the supplementary information.

Figure 2a shows the accurate mass measurements of fragment ions formed by CID of deprotonated 2,4-DNT (*m/z* 181). The *m/z* 116 ion (C_7H_2ON) is the main fragment ion observed, and its appearance is diagnostic of this isomer. Other fragment ions with lower abundance (less than 15 %) are also detected, i.e., *m/z* 164, *m/z* 151, *m/z* 134 and *m/z* 133. As formation of the *m/z* 116 ion is obviously a consecutive process (in total, it corresponds to a "H_3O_3N" loss from *m/z* 181), some of these fragment ions may serve as intermediates in the dissociation process. But, because of their low abundances, we have not been able to perform multistage MS experiments on these fragment ions. Nonetheless, the mechanism of *m/z* 116 formation can still be probed by theoretical calculations. First of all, knowing the *m/z* 116 elemental formula (C_7H_2ON), we started by considering all possible structures for this ion. Results are presented in Figure S1 in Supplementary Information (SI). One open-ring structure appears clearly to be more stable than the others: $\mathbf{M_{116\text{-}1}}$ (**Figure 1b**). The pathway leading to $\mathbf{M_{116\text{-}1}}$ starting from $\mathbf{M_{181\text{-}1}}$ requires consecutive dissociations, and different pathways have been envisaged as summarized in **Scheme 2**, based on the hypothesis that intermediates were formed *by losses* of $HO^{\bullet}$ or H_2O or $NO^{\bullet}$ (which are the most common neutral entities to be released from this type of system). To reduce the number of pathways to be considered, we have rationally limited the calculations to the dissociation steps leading to observed fragment ions. Hence, the *m/z* 181 ion may lose either $NO^{\bullet}$ (**Figure 3a**) or $HO^{\bullet}$ (**Figure S3a**) to form *m/z* 151 and *m/z* 164 ions, respectively. Results show that both are energetically possible. The $NO^{\bullet}$ loss indeed proceeds first *via* a NO_2/ONO

isomerization from the NO_2 group in *para* position (transition structure **TS1** located 242 kJ/mol above the parent ion, **Figure 3a**) followed by a barrierless $NO^{\bullet}$ elimination leading to the *m/z* 151 ion ($\mathbf{M_{151\text{-}1}}$, 66 kJ/mol). It should be noted that isomerization of the *ortho* NO_2 group was also tested (SI, **Figure S2**) and it is energetically favored compared to the *para* NO_2 isomerization, but to rationalize formation of *m/z* 116, only the *para* NO_2 isomerization pathway was viable. Furthermore, loss of $HO^{\bullet}$ from *m/z* 181 was also investigated and it involved two reasonable barriers (**TS10** and **TS11,** respectively**,** 167 and 181 kJ/mol above *m/z* 181 **Figure S3a**, SI) consisting of a ring closure and a proton-transfer leading to the $\mathbf{M_{164\text{-}1}}$ ion upon $HO^{\bullet}$ elimination.

Starting from the first line of potential intermediates (*m/z* 151 or *m/z* 164), four follow-up reactions can be considered: either a H_2O or a $NO^{\bullet}$ loss from the *m/z* 164 ion, or a $HO^{\bullet}$ or a H_2O loss from the *m/z* 151 ion, leading respectively to the ions at *m/z* 146, *m/z* 134, or *m/z* 133 (**Scheme 1**). As no *m/z* 146 ion was observed in the CID spectrum (**Figure 2a**), loss of water from *m/z* 164 was discarded. Formation of the *m/z* 134 ion occurs *via* elimination of either $NO^{\bullet}$ from *m/z* 164 or $HO^{\bullet}$ from *m/z* 151. Both pathways have been probed and each was dismissed due to the very high endothermicity of the reactions (+348 kJ/mol for $NO^{\bullet}$ loss (SI, **Figure S3b**) and > 500 kJ/mol for the $HO^{\bullet}$ release, not shown). The last possibility for this second step is formation of *m/z* 133 ion by H_2O loss from *m/z* 151. The resulting potential energy diagram is presented in **Figure 3b**. This reaction is a stepwise process, which entails intermediates with different backbones: tri-substituted phenyl, anthranil or linear. The reaction proceeds first by a cyclization which further enables the transfer of an oxygen atom of the *ortho* NO_2 group to the methylene group ($\mathbf{M_{151\text{-}3}}$). Two proton transfers then occur leading to the ion-dipole complex $\mathbf{M_{151\text{-}3}}$ which undergoes a barrierless H_2O loss. The resulting $\mathbf{M_{133\text{-}1}}$ ion has an anthranil-like backbone and easily rearranges to form the more stable $\mathbf{M_{133\text{-}3}}$ ion. Several barriers are involved in this process, and all have reasonable heights (transition structures **TS2** to **TS7** with relative energies ranging from 71 to 212 kJ/mol).

Thus, as consecutive losses of $NO^{\bullet}$ and H_2O seem to be the most favorable pathway for the two first steps of the reaction, the remaining one should consist of a $HO^{\bullet}$ elimination leading to the *m/z* 116 ion. From $\mathbf{M_{133\text{-}3}}$, it proceeds *via* the **TS8** transition structure and costs 193 kJ/mol (relatively to the starting ion $\mathbf{M_{181\text{-}1}}$, **Figure 3c**) leading to the formation of the very stable $\mathbf{M_{133\text{-}4}}$ ion (relative energy -72 kJ/mol). From there, a barrierless $HO^{\bullet}$ elimination finally leads to the $\mathbf{M_{116\text{-}1}}$ ion (+ 280 kJ/mol compared to $\mathbf{M_{181\text{-}1}}$).

Finally to validate the structure proposed for the *m/z* 116 ion, we have performed a sequential MS^3 experiment: CID of *m/z* 116 formed from *m/z* 181 shows that this ion easily ejects only CO (**Figure 2b**). From $\mathbf{M_{116\text{-}1}}$, decarbonylation is calculated to be a barrierless process leading to $\mathbf{M_{88\text{-}1}}$with a cost of 168 kJ/mol (SI, **Figure S4**). This agrees well with the experimental observation.

In conclusion, this work illustrates well the complementarity between experimental mass spectrometry with high resolution accurate mass measurements and DFT calculations. Both the experimental and theoretical approaches are indeed required to elucidate this consecutive dissociation process mechanism. Beyond the fundamental interest of this mechanistic study, more insights may also be gained by those involved in the analysis of nitroaromatic compounds.

Acknowledgements

The authors would like to thanks the commissariat à l'énergie atomique et aux énergies alternatives (CEA), SMP^3 consortium and University Pierre and Marie Curie (UPMC) for the financial support of this project. Dr. Derat is gratefully acknowledged for giving access to calculation cluster.

References

[1] K. S. Ju, R. E. Parales, *Microbiol. Mol. Biol. Rev.* **2010**, *74*, 250.
[2] J. Xu, N. Jing, *J. Hazard. Mater.* **2012**, *203-204*, 299.
[3] D. Kalderis, A. L. Juhasz, R. Boopathy, S. Comfort, *Pure Appl. Chem.* **2011**, *83*, 1407.
[4] J. Yinon, *J. Chromatogr. A* **1996**, *742*, 205.
[5] a) Y. McAvoy, K. Dost, D. C. Jones, M. D. Cole, M. W. George, G. Davidson, *Forensic Sci. Int.* **1999**, *99*, 123; b) L. Song, A. D. Wellman, H. Yao, J. E. Bartmess, *J. Am. Soc. Mass Spectrom.* **2007**, *18*, 1789; c) L. Song, J. E. Bartmess, *Rapid Commun. Mass Spectrom.* **2009**, *23*, 77.
[6] A. Schwarzenberg, H. Dossmann, R. B. Cole, X. Machuron-Mandard, J.-C. Tabet, *J. Mass Spectrom.* **2014**, *accepted for publication*.
[7] J. F. Garcia-Reyes, J. D. Harper, G. A. Salazar, N. A. Charipar, Z. Ouyang, R. G. Cooks, *Anal. Chem.* **2011**, *83*, 1084.
[8] Gaussian 09, Revision B.01, M. J. Frisch, G. W. Trucks, H. B. Schlegel, G. E. Scuseria, M. A. Robb, J. R. Cheeseman, G. Scalmani, V. Barone, B. Mennucci, G. A. Petersson, H. Nakatsuji, M. Caricato, X. Li, H. P. Hratchian, A. F. Izmaylov, J. Bloino, G. Zheng, J. L. Sonnenberg, M. Hada, M. Ehara, K. Toyota, R. Fukuda, J. Hasegawa, M. Ishida, T. Nakajima, Y. Honda, O. Kitao, H. Nakai, T. Vreven, J. A. Montgomery, J. E. Peralta, F. Ogliaro, M. Bearpark, J. J. Heyd, E. Brothers, K. N. Kudin, V. N. Staroverov, R.

Kobayashi, J. Normand, K. Raghavachari, A. Rendell, J. C. Burant, S. S. Iyengar, J. Tomasi, M. Cossi, N. Rega, J. M. Millam, M. Klene, J. E. Knox, J. B. Cross, V. Bakken, C. Adamo, J. Jaramillo, R. Gomperts, R. E. Stratmann, O. Yazyev, A. J. Austin, R. Cammi, C. Pomelli, J. W. Ochterski, R. L. Martin, K. Morokuma, V. G. Zakrzewski, G. A. Voth, P. Salvador, J. J. Dannenberg, S. Dapprich, A. D. Daniels, Farkas, J. B. Foresman, J. V. Ortiz, J. Cioslowski, D. J. Fox, Wallingford CT.

[9] a) J. P. Perdew, K. Burke, M. Ernzerhof, *Phys. Rev. Lett.* **1996**, *77*, 3865; b) N. C. Handy, A. J. Cohen, *Mol. Phys.* **2001**, *99*, 403.

[10] I. Fernandez, G. Frenking, E. Uggerud, *J. Org. Chem.* **2010**, *75*, 2971.

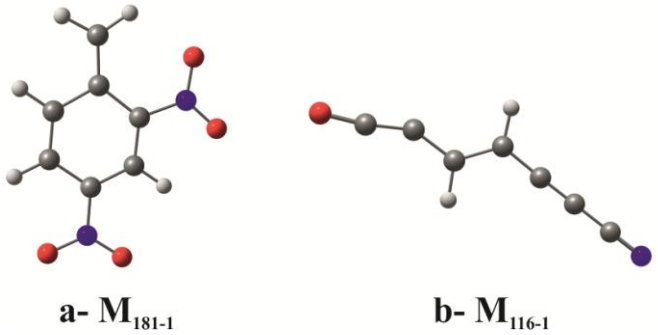

Figure 1. Optimized geometries of the most stable isomeric forms of a- *m/z* 181 from deprotonated 2,4-DNT and b- *m/z* 116 ions.

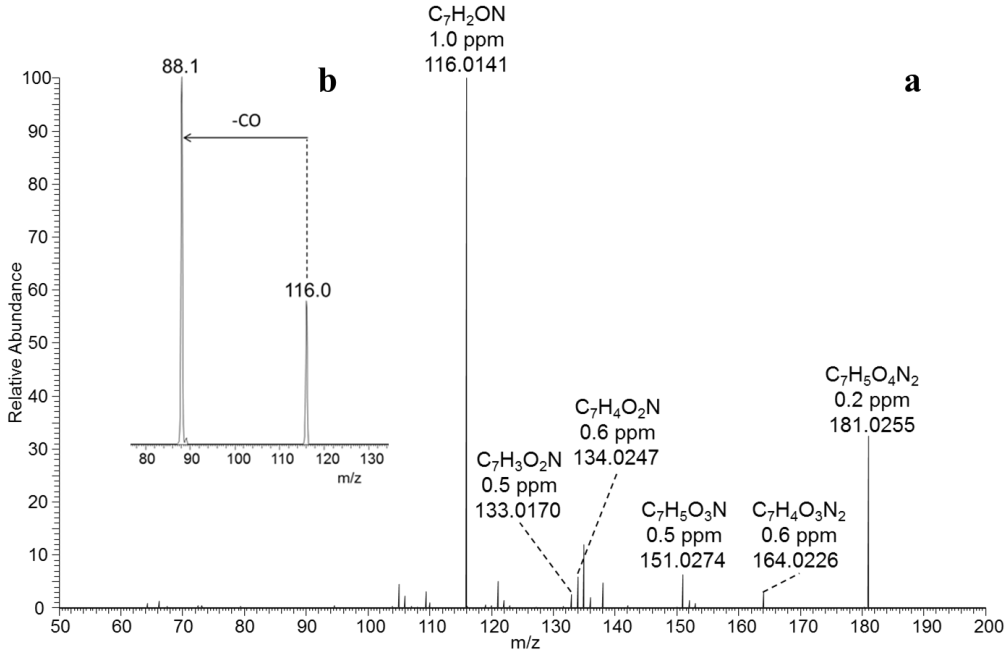

Figure 2. CID of deprotonated 2,4-DNT: a- ESI-HRMS/MS of *m/z* 181 at 35% NCE acquired in Orbitrap, b- ESI-MS^3 of *m/z* 116 at 20% NCE acquired in the LTQ.

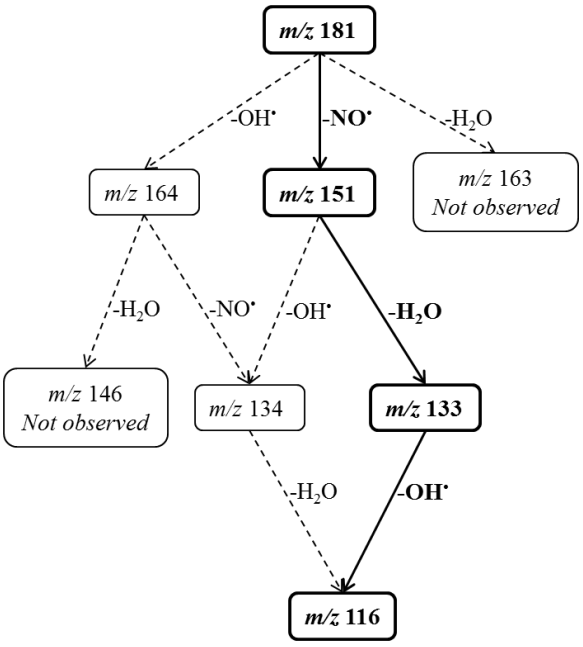

Scheme 1. Various possible dissociation pathways of the *m/z* 181 ion leading to the *m/z* 116 ion. The retained pathway is indicated by the solid black lines.

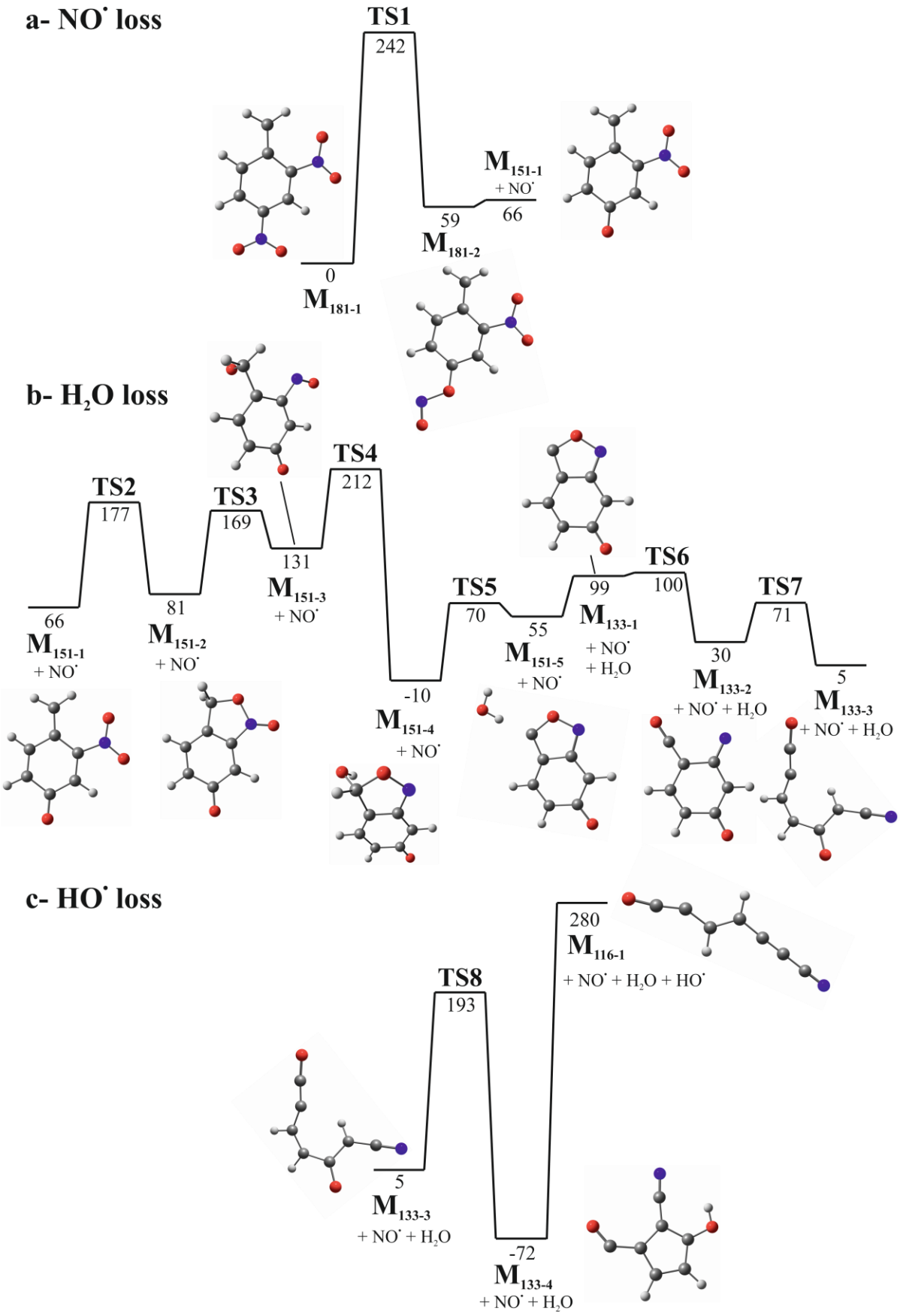
a- NO˙ loss
TS1
242
M151-1
+ NO˙
59
66
M181-2
0
M181-1
b- H2O loss
TS2
177
TS3
169
TS4
212
131
M151-3
+ NO˙
66
M151-1
+ NO˙
81
M151-2
+ NO˙
-10
M151-4
+ NO˙
TS5
70
55
M151-5
+ NO˙
TS6
100
99
M133-1
+ NO˙
+ H2O
TS7
71
30
M133-2
+ NO˙ + H2O
5
M133-3
+ NO˙ + H2O
c- HO˙ loss
280
M116-1
+ NO˙ + H2O + HO˙
TS8
193
5
M133-3
+ NO˙ + H2O
-72
M133-4
+ NO˙ + H2O

Figure 3. Potential energy diagram for the multistep dissociation pathway: a- $NO^{\bullet}$ loss and b- H_2O loss and c- $HO^{\bullet}$ loss (relative energies (E_{rel}) in kJ/mol).